R-06-95

Stress variations during a glacial cycle at 500 m depth in Forsmark and Oskarshamn: Earth model effects

Björn Lund, Department of Earth Sciences,
Uppsala University

June 2006

Svensk Kärnbränslehantering AB
Swedish Nuclear Fuel
and Waste Management Co
Box 5864
SE-102 40 Stockholm Sweden
Tel 08-459 84 00
+46 8 459 84 00
Fax 08-661 57 19
+46 8 661 57 19

ISSN 1402-3091
SKB Rapport R-06-95

Stress variations during a glacial cycle at 500 m depth in Forsmark and Oskarshamn: Earth model effects

Björn Lund, Department of Earth Sciences,
Uppsala University

June 2006

Summary

A nuclear waste repository in Sweden will, most likely, have to endure one or more glaciations during the course of its life time. In order to estimate how the the repository will be affected by stresses induced by a glaciation, we perform modeling where the ice sheet history is one important aspect and the mechanical properties of the Earth another. Often very simplified models of the Earth are used in these modeling efforts and the purpose of the present study is to investigate how increasing complexity of the Earth model affect the resulting stresses at a repository depth of 500 m.

In this study, I use two-dimensional Earth models which are tested with two different ice histories, one very simplified model of a two-dimensional, elliptic cross-section ice sheet and one complex simulation of the previous, the Weichselian, Fennoscandian glaciation. For the simple ice model, stresses are estimated along a profile from the center of the ice sheet out past the ice edge in order to facilitate interpretation. For the Weichselian ice model, stresses are estimated only at the proposed repository sites at Forsmark and Oskarshamn. The estimated stresses for some of the models are finally used to estimate fault stability during a glacial cycle at the proposed sites.

The Earth models in this study are based on a very simple model with a viscoelastic half-space overlain by a 100 km thick elastic plate. The complexity of the model is then increased by introducing horizontal layers in both the elastic plate, which always remain elastic to 100 km depth, and in the viscoelastic half-space. In these layers I vary the elastic parameters Young's modulus, Poisson's ratio and density. I have also included variations in the viscosity structure of the half-space.

I find that as the complexity of the models increase, and the properties of the uppermost kilometer of the Earth become less affected by average properties from deeper down, the flexural stresses at 500 m depth decrease, as expected. A lower Young's modulus, lower compressibility and lower density in the uppermost layer all act to lower the stresses. However, the three properties act differently on the resulting response. Introducing layering in Young's modulus generally decreases the stresses all along a profile through the ice model. Going from incompressible to compressible models affect the stresses outside the ice edge significantly more than the stresses under the ice sheet. Introducing layering in density conversely affect the stresses under the ice sheet more than those outside the ice edge. The combined effects of the most complex models tested here show that the glacially induced horizontal stresses at 500 m depth decrease to levels very similar in magnitude to the loading stress. There are, however, temporal variations in these horizontal stresses that do not follow the loading stress and which induce tensional or compressional horizontal stresses that persist when no ice is present.

As is well known, changes in viscosity structure has a very large effect on the Earth response. Viscosity affect both the magnitudes of the induced stresses and the temporal behavior of the stress evolution. This is confirmed in the current study. Large effects on the Earth's response is also expected from the inclusion in the models of three-dimensionality in ice and Earth structure, sea-level changes, errors in the ice model etc, none of which has been considered in this study.

The glacially induced stresses for some of the models have been used in combination with the current background stress field at Forsmark and Oskarshamn to evaluate fault stability throughout a glacial cycle. The results show that with the used ice model and Earth models, fault stability is generally enhanced in both Forsmark and Oskarshamn during ice cover of the sites. Oskarshamn, however, show long periods of decreased fault stability during inter-stadials and for some models at the end of the final deglaciation. Fault stability in Forsmark is generally higher than in Oskarshamn, with the exception of a pulse of instability at the end of deglaciations. The stability analysis did, however, not include a pore pressure analysis, which is crucial to include at a later stage.

Contents

1 Introduction

In the design of a deep bedrock nuclear waste repository, great care has to be taken to evaluate the mechanical loads that the construction may experience. Due to the long time frames involved in the radioactive decay of spent nuclear fuel, it is very likely that a repository in Sweden will have to endure one or more glaciations. The purpose of this study is to investigate how different one-dimensional models of the Earth responds to a glaciation and to obtain a range of characteristic stress data at repository depth in the crust, within the limitations of the modeling. In this report I first use a simple elliptic cross-section ice sheet model in order to show the characteristics of the Earth's response. Then a full simulation of the Weichselian ice sheet is used to study how a typical glaciation induces stresses at Forsmark and Oskarshamn. The modeling is performed along an almost north-south trending two-dimensional profile through the three-dimensional Weichsel ice model, with the profile going through the proposed repository sites of Forsmark and Oskarshamn. The report ends with estimates of fault stability at Forsmark and Oskarshamn during the glaciation, using both the induced glacial stresses and representative background stresses at the two sites.

1.1 Modeling glacial isostatic adjustment

Techniques and methods for the modeling of glacial isostatic adjustment (GIA) has developed rapidly during the last decade. Traditionally based on spectral decomposition in relaxation modes e.g. /Peltier 1974, Wu and Peltier 1982, Wolf 1991/, the current move to incorporate lateral variations in the Earth's composition, its spherical shape and gravitation has lead to the adaption of various finite element techniques e.g. /Martinec 2000, Wu and van der Wahl 2003, Wu 2004, Latychev et al. 2005/. Other efforts have been directed to incorporating the effects of changing sea-levels and the rotation of the Earth e.g. /Johnston 1993, Milne and Mitrovica 1998, Mitrovica et al. 2001/ and investigations into the effects of compressibility on GIA predictions e.g. /Han and Wahr 1995, Klemann et al. 2003/.

Since the observables in glacial rebound are mostly related to displacements of the Earth's surface, usually in the form of relative sea-level measurements such as e.g. raised beaches or tide-gauge data but today increasingly in the form of GPS-measurements, most of the GIA modeling results are presented as displacements. Notable exceptions to this is found in e.g. /Johnston et al. 1998, Klemann and Wolf 1998, 1999, Ivins et al. 2003/, which all show the stresses induced by the studied glacial loads. These studies constitute good verification sources for my implementation of GIA modeling.

In this report I use a finite element methodology based on /Wu 1992, 2004/ which allows for the inclusion of pre-stress advection into a commercial finite element package; I use Abaqus /Abaqus 2004/. The approach does not include a full treatment of compressibility, the so called internal buoyancy term in the full momentum equation, but does take material compressibility into account /Wu 2004, Klemann et al. 2003/. The methodology was reviewed in /Lund 2005a/ where verifications of the modeling scheme were presented. Further verification efforts are currently in progress. With Volker Klemann at the GeoForschungs Zentrum, Potsdam, Germany, we compare finite element and spectral calculations for compressible viscoelastic Earth models and with Erik Bängtsson and Maya Neytcheva at the Department of Scientific Computing, Uppsala University we compare different finite element implementations of pre-stress advection for elastic compressible models. These tests have, however, not been finished in time for this report but will be reported on at a later time. The Earth models in this report are two-dimensional, plane strain finite element models which use infinite elements on the lower and side boundaries.

2 Ice sheet models

In this study of glacially induced stresses I will use two different ice sheet models in order to investigate the response of the Earth models. First a geometrically simple ice model will be used to illuminate the main characteristics of the Earth response, then a detailed ice model of the Weichselian glaciation will be used to estimate representative stress time histories.

2.1 A two-dimensional elliptical ice sheet

I first use a very simple two-dimensional ice model with an elliptical cross-section which is 900 km from center to rim and is stationary, i.e. the ice grows concurrently over the 900 km and only in height, see Figure 2-1. The ice sheet grows linearly from nothing to 2.8 km height at the center in 90,000 years, to the Last Glacial Maximum, and then disappears linearly in 10,000 years. The modeling continues another 8,000 year to simulate the Holocene up until today. With a density of 917 kg/m^3, the ice sheet produces a load of 25 MPa at the center, which decays elliptically to the rim of the ice sheet as $l = L\sqrt{1-(r/R)^2}$ where l is the ice load at distance r from the center and L and R are the load at the center and the total distance from center to rim, respectively.

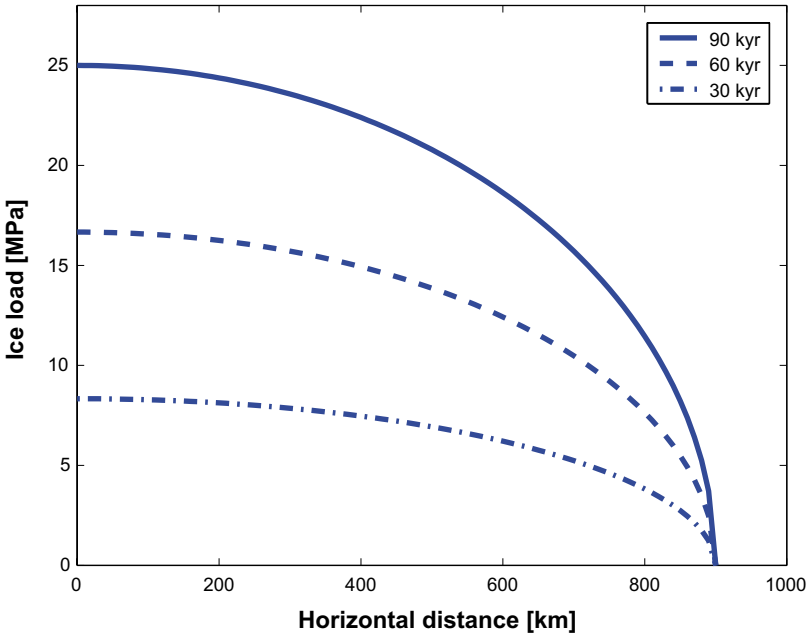

Figure 2-1. *Two-dimensional elliptic cross-section ice profile used in the modeling. Load distributions for the ice sheet during the growth phase at 30 kyr, 60 kyr and 90 kyr is shown by the blue lines.*

2.2 Model of the latest Fennoscandian glaciation

In order to model the Earth's response to a more realistic representation of a Fennoscandian glaciation I use the UMISM model by /Näslund 2006/, which is also the reference glacial cycle simulation of the Swedish Nuclear Fuel and Waste Management Co. (SKB) /SKB 2006b/. The model spans the time period from 120 kyr BP until today and includes a simulation of the entire Weichselian ice sheet. The model resolution is 50×50 km and for the current study I extracted a 2D profile striking N14.9°E through the ice model, see Figure 2-2. Note that the profile does not follow the 14.9° meridian but has a 14.9° angle to the meridian through the southernmost point on the profile. I only used the ice history from 68 kyr BP as the early stages of the ice history are rather uncertain (Näslund 2006, personal communication).

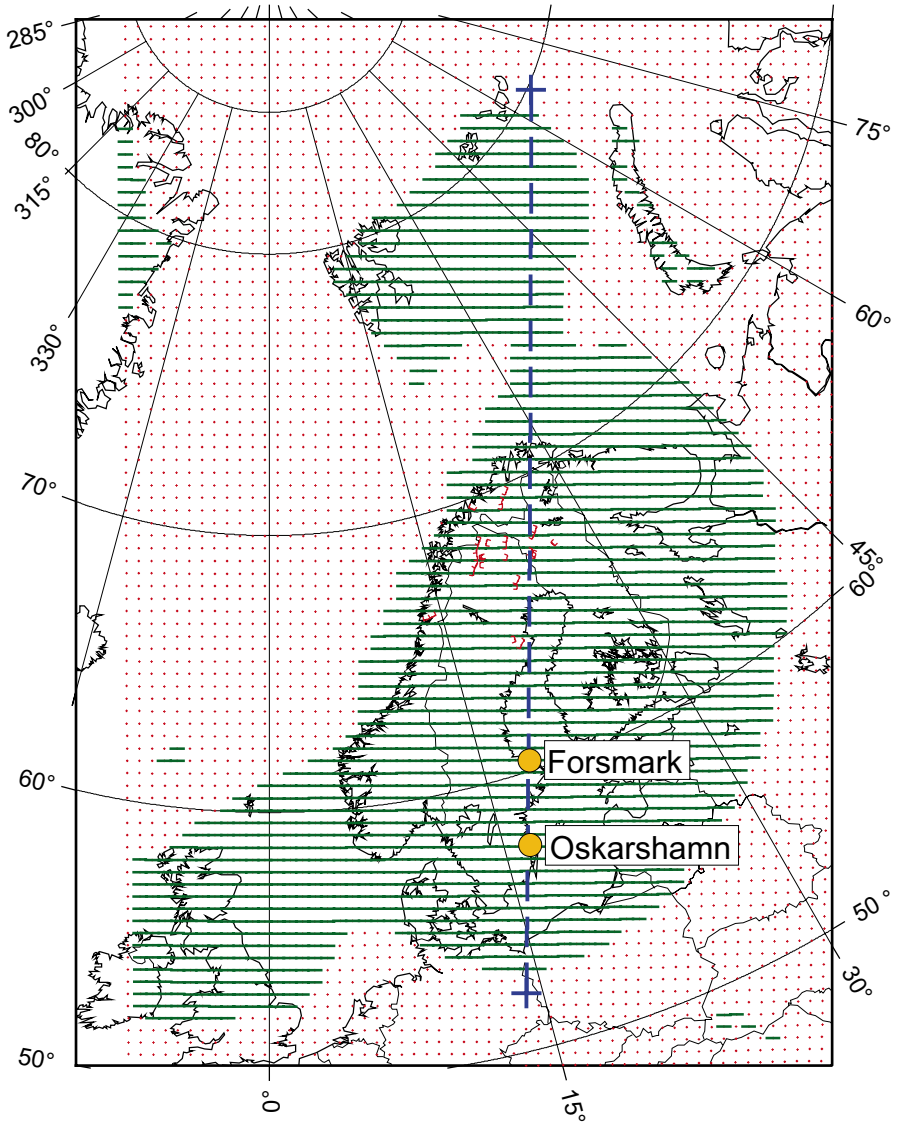

Figure 2-2. *The Weichselian ice sheet simulation by /Näslund 2006/ at 18.4 kyr BP when the ice has its largest extent along the 2D modeling profile (blue). The ice cover is indicated by green lines, the large end-glacial faults of northern Scandinavian in red and the proposed nuclear waste repository sites, Forsmark and Oskarshamn, have been marked on the map. Red dots indicate the grid used by /Näslund 2006/.*

Figure 2-3 shows the ice time histories at Forsmark and Oskarshamn, we see that the ice reaches almost 3 km thickness over Forsmark and almost 2.5 km thickness over Oskarshamn. The ice cover over Forsmark also last for a longer time period than it does over Oskarshamn. During the stadial at approximately 60 kyr BP the difference in ice coverage at Forsmark and Oskarshamn is especially noticeable, we will see the effect of this later in the modeling results. Figure 2-3 also includes a recent ice model by /Lambeck 2005/. We see that there are pronounced differences in both the thickness of the ice cover at LGM, and the duration of the stadials. The /Lambeck 2005/ model will be discussed in section 5 below.

Climate driven ice sheet models such as /Näslund 2006/ and a multitude of empirical data such as shore-line displacements, lake-level data, glacial moraines etc provide evidence that there is good reason to believe that a future glaciation will not be fundamentally different to the latest glaciation. In the modeling below I will use the /Näslund 2006/ ice model as an example of a typical Fennoscandian glaciation and commence the next ice age 2,000 years from the present. I will therefore model 2 plus 68 kyr ahead, until 70 kyr After Present (AP).

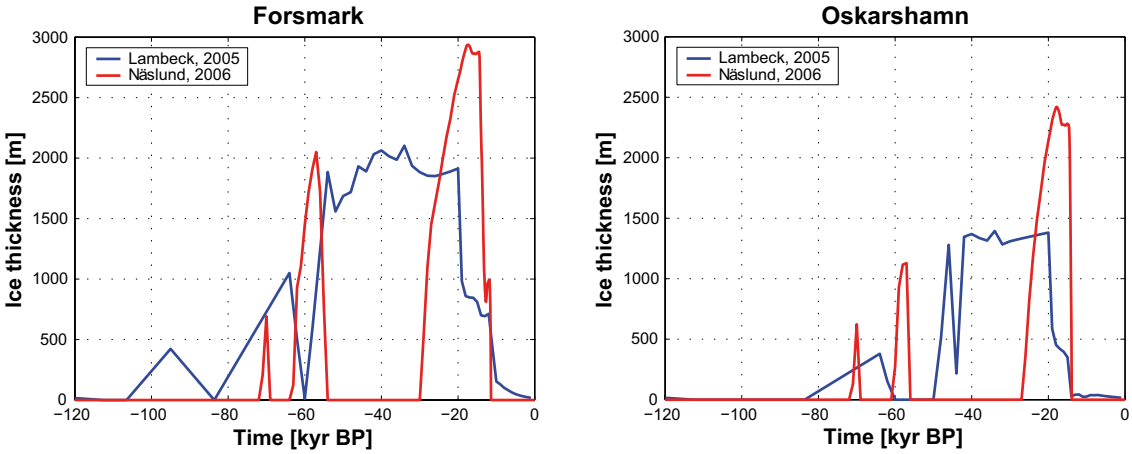

Figure 2-3. *Ice thickness histories at Forsmark, left, and Oskarshamn, right. In red the ice sheet simulation by /Näslund 2006/ and in blue the simulation by /Lambeck 2005/. The small peak at approximately 70 kyr BP in the /Näslund 2006/ simulation will not be used in the modeling in this study due to its uncertainty (Näslund 2006, personal communication).*

3 Solid earth models

The main focus of this report is on a study of how variations in the Earth model affects the resulting stresses. I have tested a number of different Earth models, all based on the concept of an elastic plate overlying a viscoelastic substratum. Increasing complexity is added to the model by introducing uniform horizontal layers of varying elastic properties and by varying the viscosity of the substratum. The elastic properties I use are Young's modulus, Poisson's ratio and the density. Each Earth model is tested both with the simple, elliptical ice sheet, in order to understand the basic response to the load, and the simulated Weichselian glaciation in order to determine the Earth model's response to a proper glaciation.

The reference Earth model in this study, model A0, is the same as that used in /Lund 2005a/, which in turn is based on the model in /Klemann and Wolf 1998/. It has a 100 km thick elastic lithosphere overlying a viscoelastic half-space. The elastic plate has Young's modulus $E = 192$ GPa and density $\rho = 3{,}380$ kg/m^3, the viscoelastic half-space has $E = 435$ GPa, $\rho = 3{,}380$ kg/m^3 and viscosity $\eta = 1 \cdot 10^{21}$ Pa s. Both layers are incompressible, $\nu = 0.5$. The following variations of the reference Earth model have been used in this study, I only list the deviations from the reference model:

One 100 km elastic layer:

A. The elastic layer is compressible, with $\nu = 0.25$.

C. The elastic layer has density $\rho = 2{,}730$ kg/m^3.

D. The elastic layer has $\rho = 2{,}730$ kg/m^3 and $\nu = 0.25$.

Two elastic layers, each 50 km thick:

E. E = 130 GPa and 254 GPa, which averages to 192 GPa, incompressible.

F. E = 130 GPa and 254 GPa, both layers with $\nu = 0.25$.

G. E = 130 GPa and 254 GPa, both layers with $\nu = 0.25$, upper layer has $\rho = 2{,}730$ kg/m^3 and lower layer has $\rho = 3{,}370$ kg/m^3.

Three elastic layers with thickness 33, 34 and 33 km, from the surface down:

H. E = 90 GPa, 196 GPa and 290 GPa, respectively, which averages to 192 GPa, incompressible.

J. E = 90 GPa, 196 GPa and 290 GPa, respectively, all three layers have $\nu = 0.25$.

K. E = 90 GPa, 196 GPa and 290 GPa, respectively, $\rho = 2{,}730$ kg/m^3, 3,370 kg/m^3 and $\rho = 3{,}380$ kg/m^3, respectively, all three layers have $\nu = 0.25$.

Viscosity variations:

KL1. As model K but with a viscosity of $5 \cdot 10^{21}$ Pa s in the half-space.

O. As model K but with two viscoelastic layers instead of one. An upper mantle from 100–670 km with viscosity $\eta = 8 \cdot 10^{20}$ Pa s and a lower mantle below 670 km with $\eta = 10^{22}$ Pa s, after /Milne et al. 2004/.

Models which use SKB site investigation data (H. Hökmark, personal communication) for an average Young's modulus (63 GPa) in the uppermost 5 km and the Preliminary Reference Earth Model (PREM) /Dziewonski and Anderson 1981/, see Figure 3-1, for Young's modulus and Poisson's ratio below 5 km, down to the core-mantle boundary. The Poisson's ratio in the upper 5 km are taken from PREM:

P. Young's moduli from SKB and PREM through the entire model, otherwise incompressible with uniform reference model density.

Q. Young's moduli and Poisson's ratios from SKB and PREM through the entire model, uniform reference model density.

During the cause of modeling it became clear that models with multiple viscoelastic layers produces results which are not in line with the results from models with a viscoelastic half-space. This behavior needs further investigation. Similarly, as will be discussed below, complicated density structures such as that in the PREM also produces deviating results which should be investigated further. Such studies are beyond the scope of the current project.

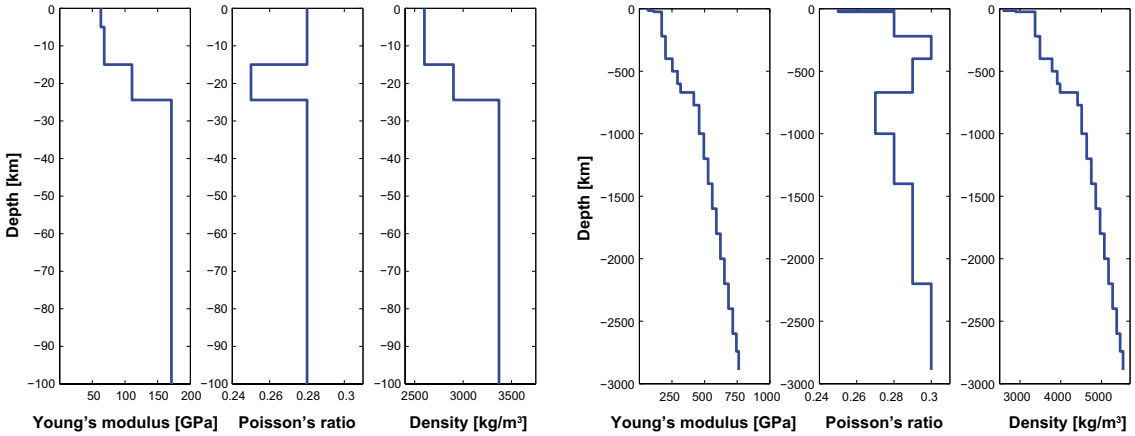

Figure 3-1. *Illustrations of the elastic parameters of the PREM /Dziewonski and Anderson 1981/ model, with Young's modulus in the upper 5 km replaced by the SKB site investigation average 63 GPa (H. Hökmark, personal communication). The left three panels show the upper 100 km of the Earth model, the right three panels show the model down to the core-mantle boundary.*

4 Results

This section is a gallery of figures of the responses of the different models to the two load scenarios. The characteristics of each model response will be described and commented on here, discussions of the results follow in the next section. Full model descriptions are in section 3 above.

The results of models with the elliptical ice sheet are presented as horizontal sections along the ice sheet, from the center out past the rim. I show three time periods; the last glacial maximum (LGM) when the ice sheet reaches maximum height, the end of glaciation (EoG) when the ice sheet has just disappeared and today (Now). The results with the forward projection of the Weichselian glaciation are presented as time histories at Forsmark and Oskarshamn, respectively, starting 2 kyr in the future (After Present) at the 68 kyr BP point in the Weichsel model. The model results are presented as the maximum and minimum horizontal stresses (SH and Sh, respectively) and the vertical stress (Sv), all evaluated at 500 m depth in the models.

4.1 Stiffness variations

We start by studying the effect of introducing layers of varying stiffness, or Young's modulus. Models A0, E, H and P are all fully incompressible, with identical density, elastic layer thickness and viscosity but with varying Young's modulus structure. The 100 km elastic plate has one layer in A0, two in E, three in H and four in P. In models A0, E and H the average stiffness over the 100 km is the same, 192 GPa, whereas in model P the stiffness averaged over 100 km is 150 GPa. Model P also has stiffness variations in the viscoelastic half-space, these however affect the results very little /Lund 2005a/.

4.1.1 Elliptical ice sheet

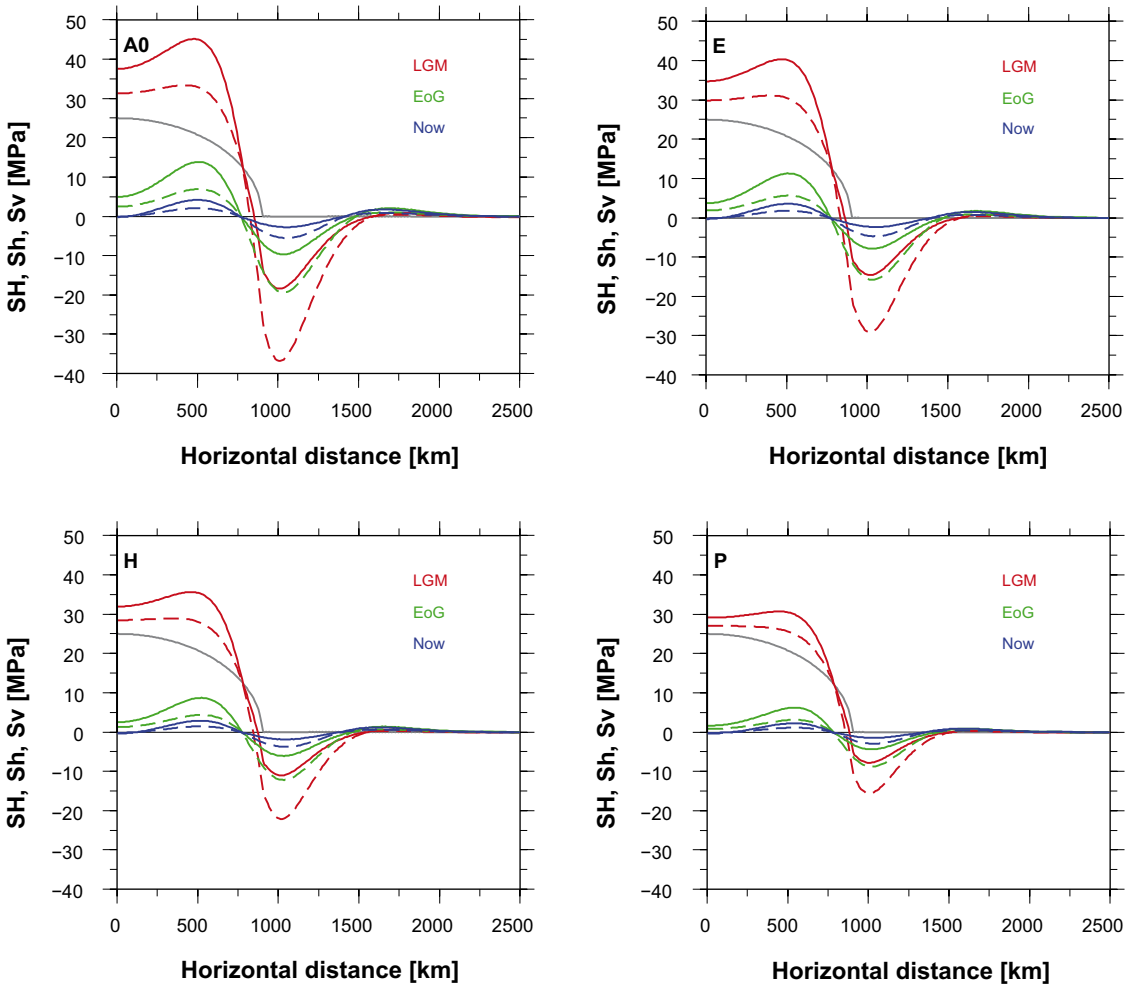

Figure 4-1. *Glacially induced stresses at three different times, LGM (red), EoG (green) and Now (blue), using a simple two-dimensional elliptical cross-section ice model. Stresses are displayed at 500 m depth in Earth models A0, E, H and P. The horizontal distance is from the center of the ice outwards. Solid lines are the maximum horizontal stresses, SH, dashed lines are the minimum horizontal stresses, Sh. The vertical stress at LGM is shown by the gray solid line (25 MPa at the center).*

4.1.2 Weichselian ice sheet

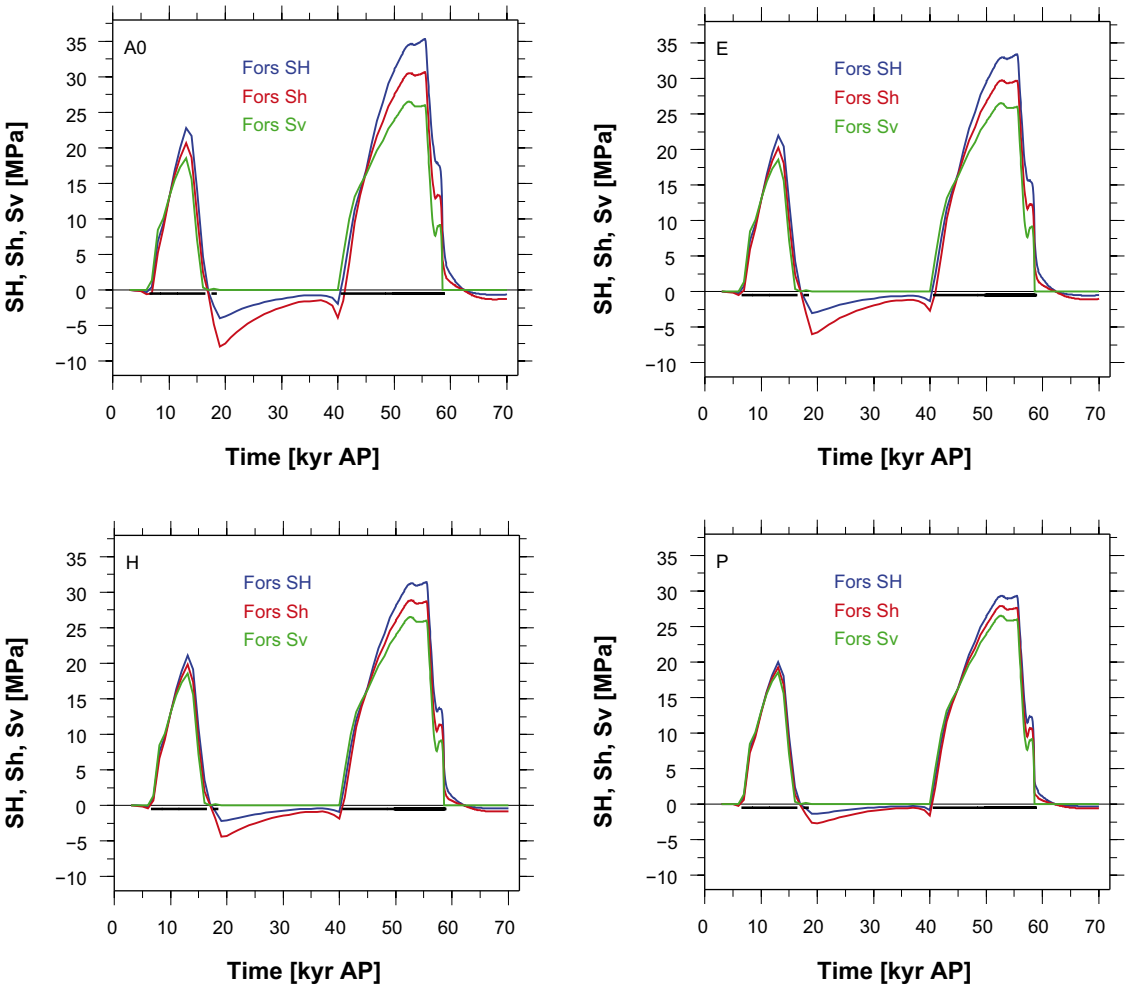

Figure 4-2. *Glacially induced stresses at 500 m depth in Forsmark, using the forward projection of the Weichselian ice sheet model. Maximum horizontal stress, SH (blue), minimum horizontal stress, Sh (red) and vertical stress, Sv (green). The black horizontal lines indicate the periods of ice cover. Earth models A0, E, H and P.*

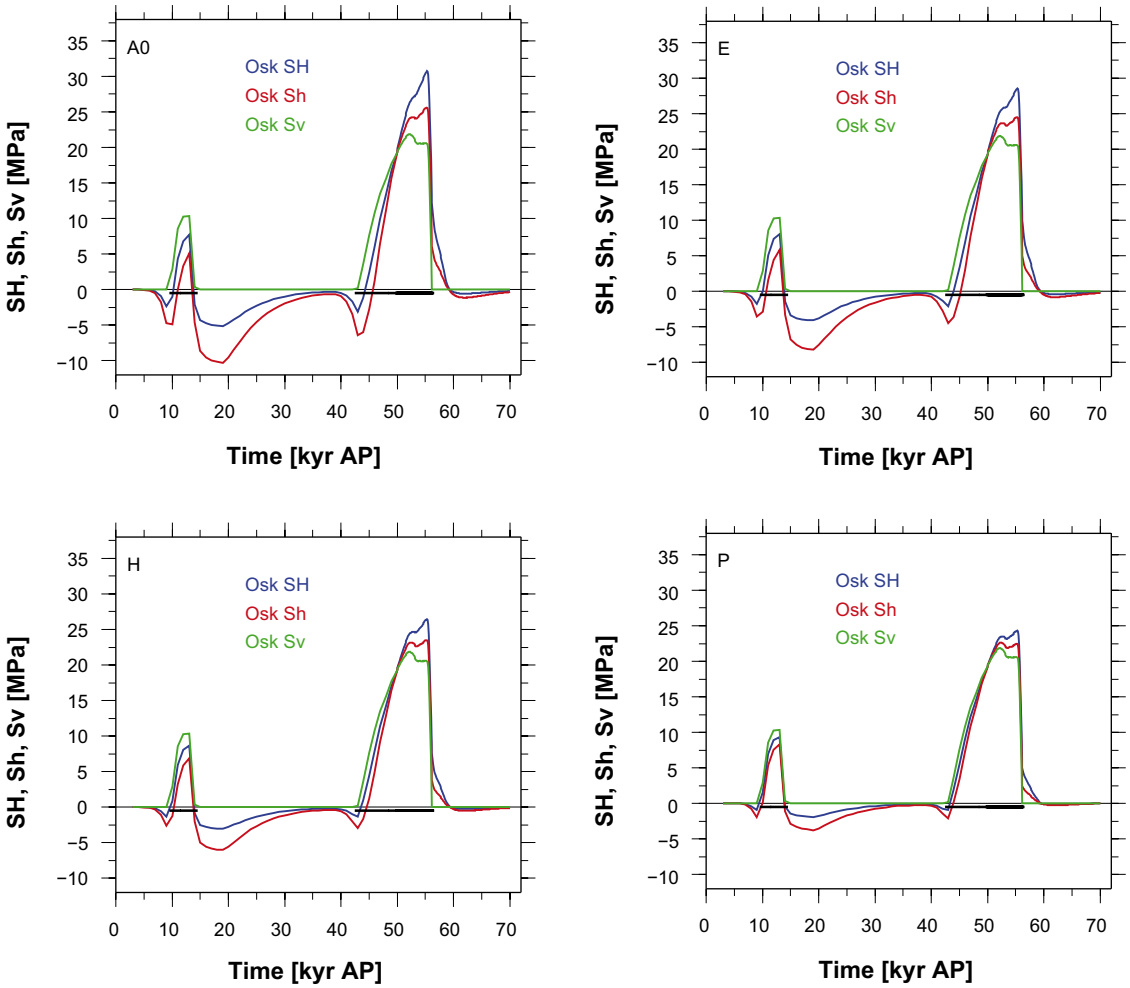

Figure 4-3. *As in Figure 4-2, but at the location of Oskarshamn.*

4.1.3 Comment

We see in Figure 4-1 that as softer layers are introduced near the surface and stiffness decreases at 500 m depth, stress magnitudes decrease as the bending of the plate induces less stress. Interestingly, the induced tensile stress outside the ice margin decreases more dramatically than the compressive stress.

Figures 4-2 and 4-3 show the same decreasing stress magnitudes as layering is introduced, especially in the stress peak at LGM, approximately 52 kyr AP. As in Figure 4-1, we notice that the horizontal stress magnitudes more and more resemble the vertical stress magnitude as more layers are introduced, also the induced tensile stress during times of no ice tends to zero. We also note that there is induced horizontal tensile stresses after the first deglaciation, at approximately 15 kyr AP, but induced horizontal compressive stresses after the LGM deglaciation.

4.2 Including compressibility

As referred to above, the modeling technique used in this study has the capability of including material compressibility into the model, but not the capability to solve the complete compressible problem, which also includes internal buoyancy (dilatancy). In other words, Hooke's law with Poisson's ratio less than 0.5 is used but the model does not consider the effects of a change in density due to compression or dilation. This issue of a technical, but unphysical, division of compressibility into two terms is further discussed by e.g. /Klemann et al. 2003/. The buoyancy term in the momentum equation counteracts the pre-stress advection term, so by neglecting it we will slightly underestimate the stresses, see /Kleman et al. 2003/.

Here I add material compressibility to the models discussed in the previous section, the results in this section are from models A, F, J and Q which all have Poisson's ratio 0.25 in the elastic plate, in addition to the stiffness variations. The viscoelastic half space is incompressible.

4.2.1 Elliptical ice sheet

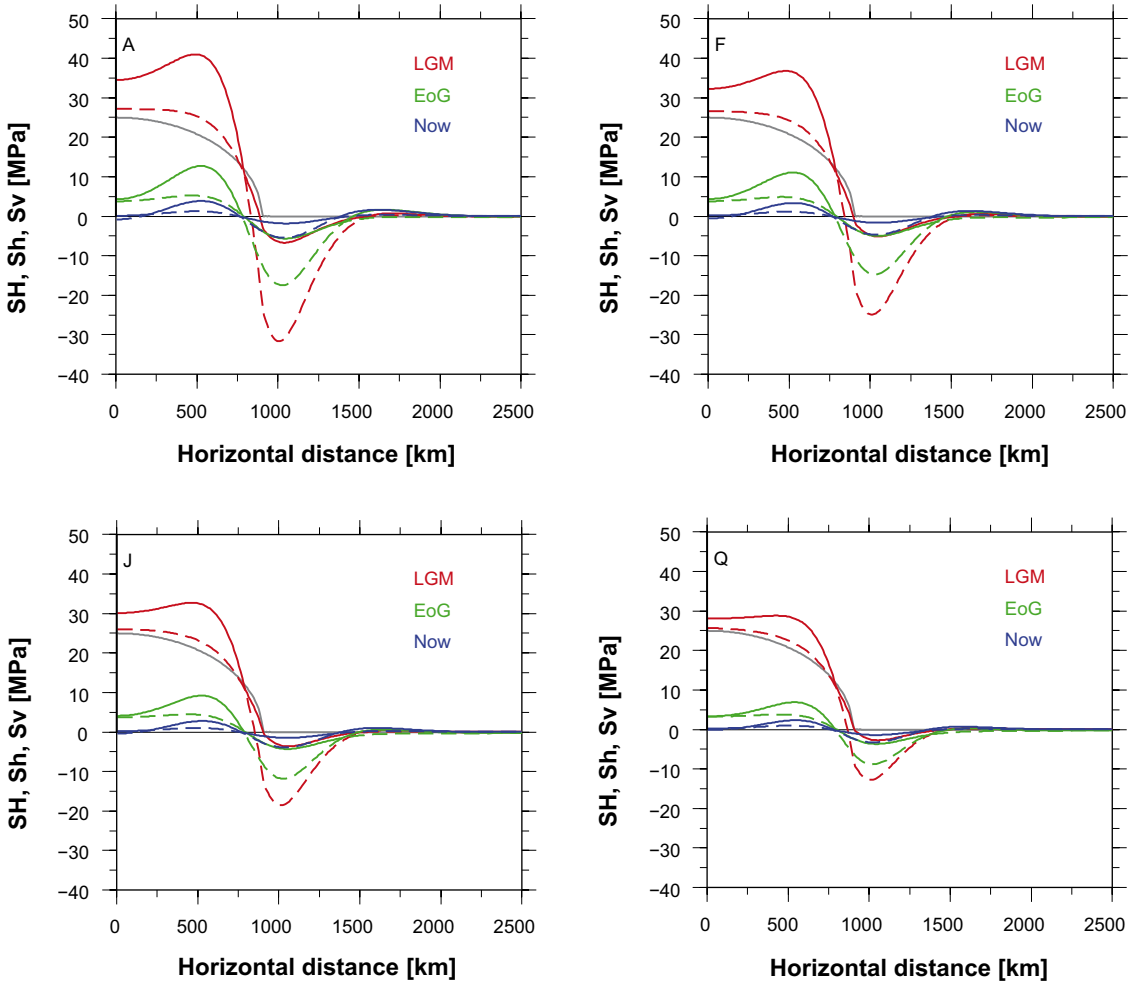

Figure 4-4. *As in Figure 4-1, but for models A, F, J and Q with compressibility, ν = 0.25 in the 100 km elastic lithosphere.*

4.2.2 Weichselian ice sheet

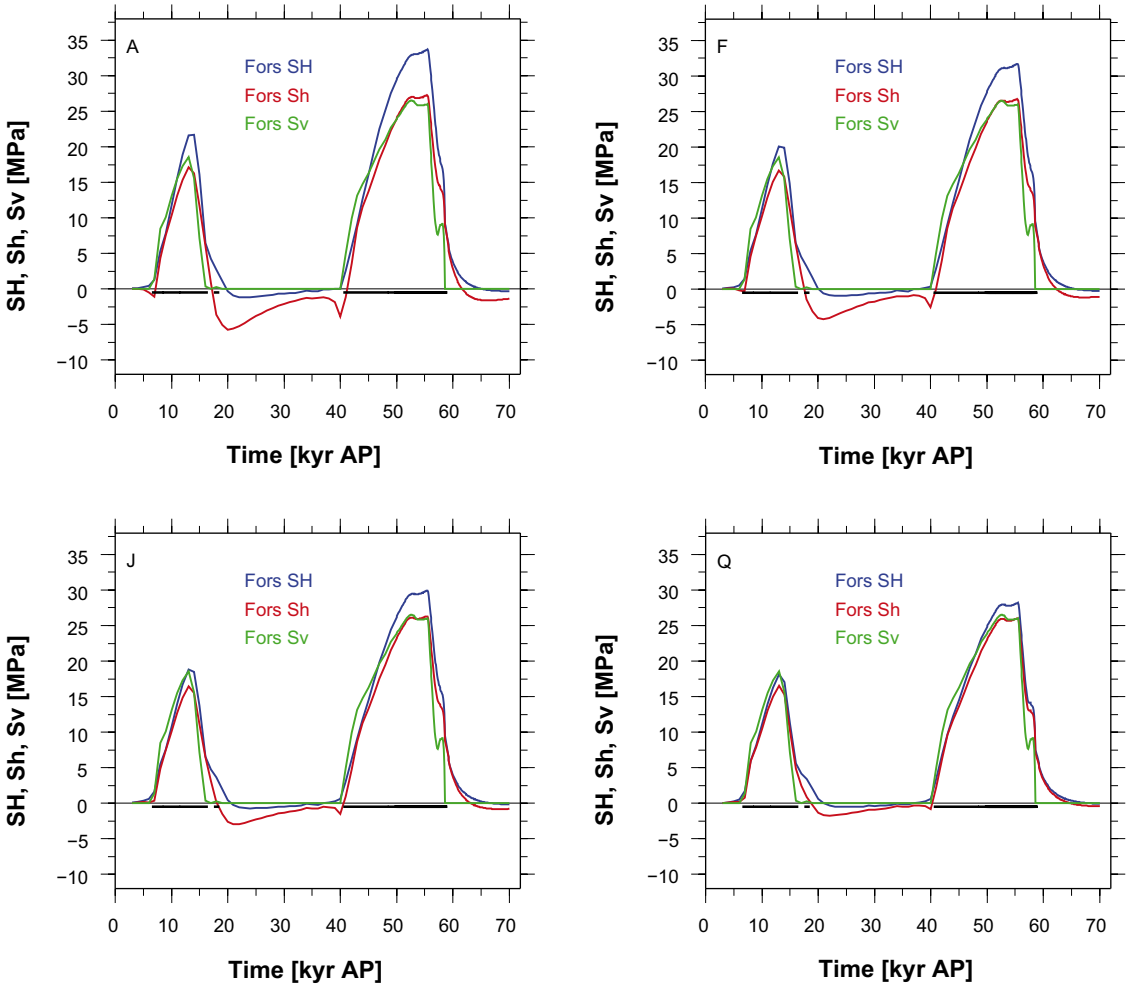

Figure 4-5. *As Figure 4-2, but for models A, F, J and Q with compressibility, ν = 0.25 in the 100 km elastic lithosphere.*

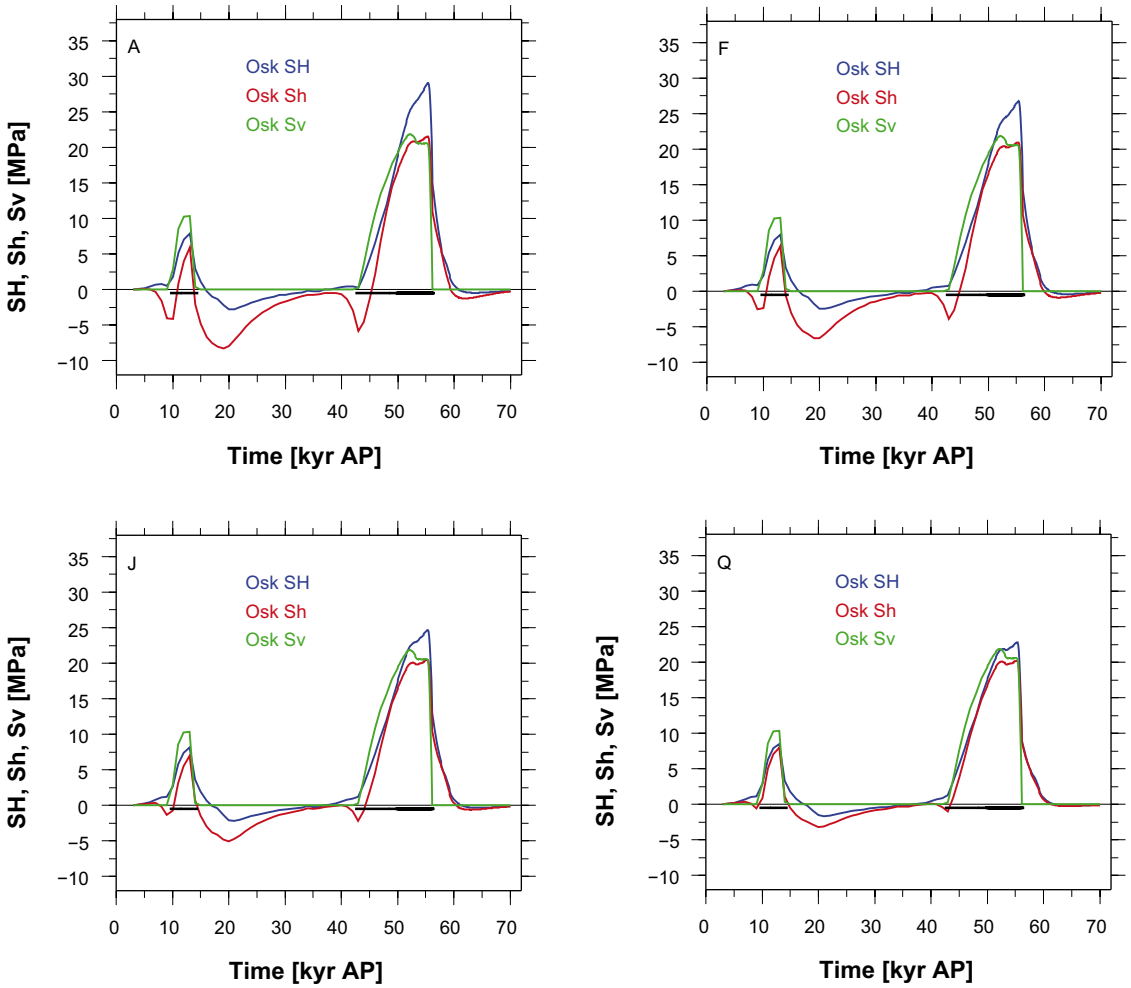

Figure 4-6. *As in Figure 4-3, but for models A, F, J and Q with compressibility, ν = 0.25 in the 100 km elastic lithosphere.*

4.2.3 Comment

Comparing Figures 4-1 and 4-4, we see that a compressible material lowers the horizontal stress magnitudes, as expected. We note that the effect is largest on the maximum horizontal stress, SH, outside the ice rim. The tensile magnitude of SH is significantly lowered by compressibility. We also note that the minimum horizontal stress, Sh, under the ice sheet at LGM now is very close in magnitude to the vertical stress.

Comparing the stress time histories at Forsmark and Oskarshamn, we again see that Sh has decreased during the glaciated periods, and that SH has increased towards zero during the inter-stadials. We also note that in these models, Sh is very rarely larger that the vertical stress. The induced compressive horizontal stresses after the LGM deglaciation are larger than in the corresponding incompressible models.

4.3 Density variations

The subject of including density variation in GIA models is a topic of some discussion, e.g. /Wu and Peltier 1982, Wu and Ni 1996, Lund 2005a/. If the density gradients observed in the Earth are modeled using volume averages, the density contrasts between the layers will be exaggerated and the buoyancy forces produced in such models may be excessively large. Here I use four simple density structures to illustrate the effect of density variations, the PREM model density structure, shown in Figure 3-1, could not be modeled with enough confidence at this time.

In this section, density variations is introduced in the models discussed above. Model C has an elastic lithosphere with density $\rho = 2{,}730$ kg/m^3 instead of the reference $\rho = 3{,}380$ kg/m^3, but is incompressible. Models D, G and K include layers of varying density, all lower than the reference density in the elastic layer, in addition to being compressible and having stiffness variations.

4.3.1 Elliptical ice sheet

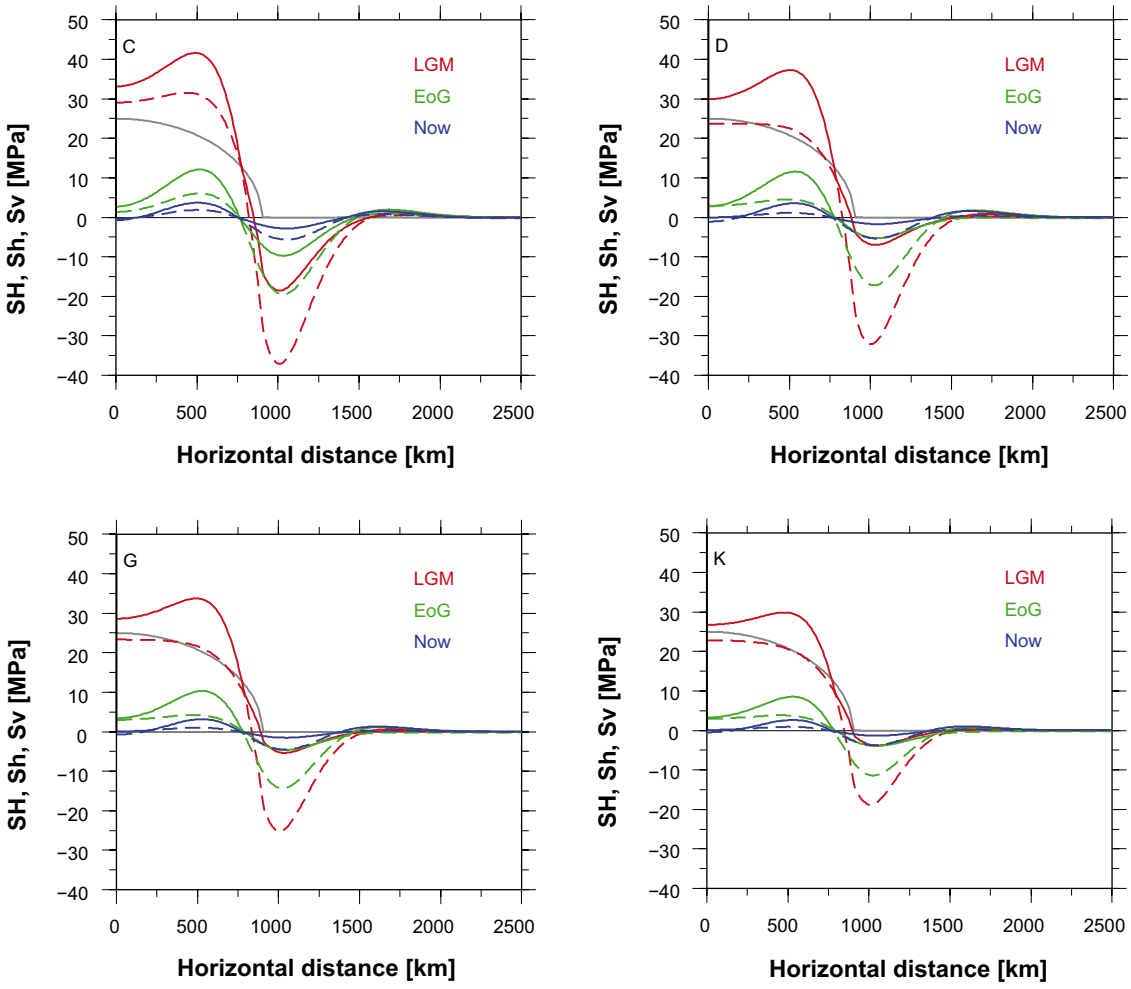

Figure 4-7. *As Figure 4-4, now with models C, D, G, and K which contain density variations.*

4.3.2 Weichselian ice sheet

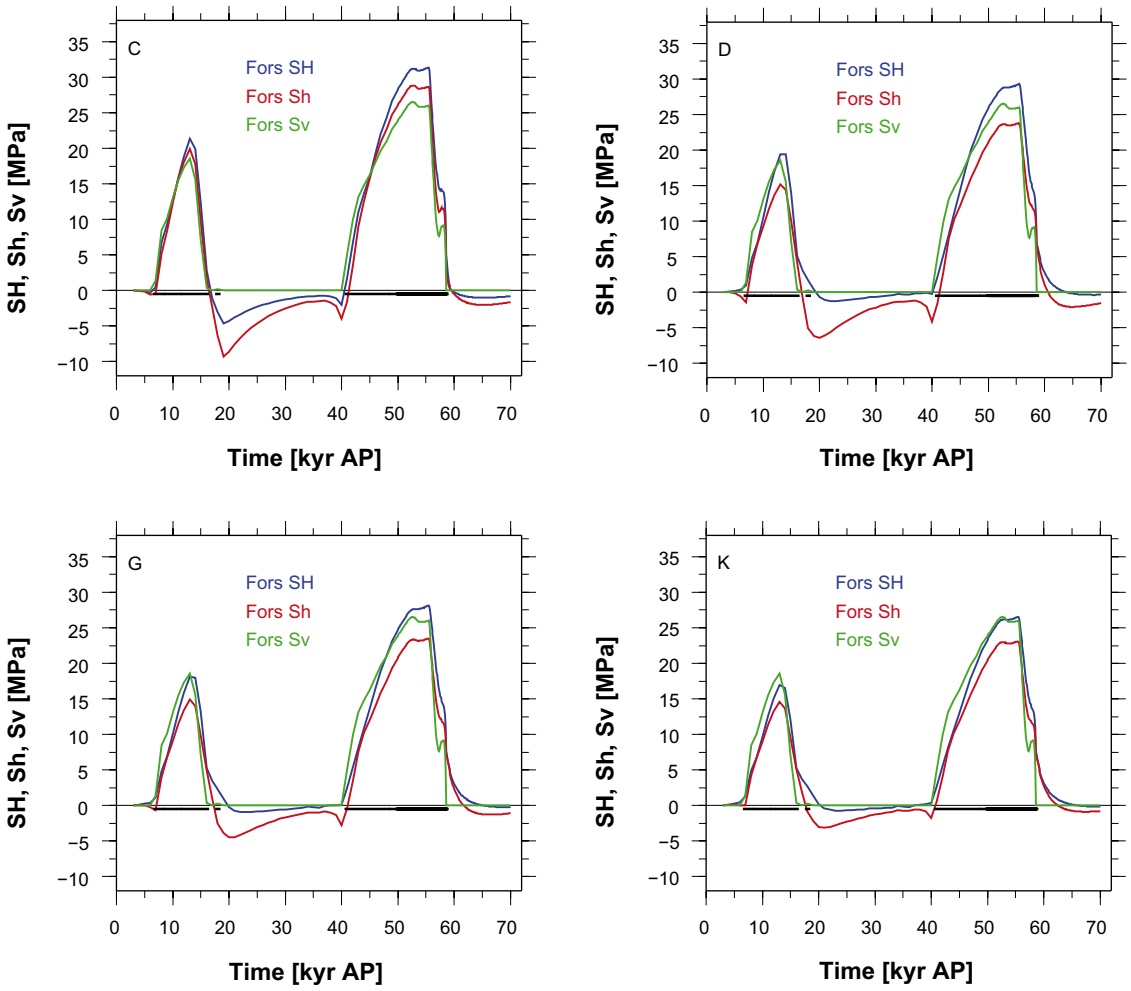

Figure 4-8. *As Figure 4-5, now with models C, D, G, and K which contain density variations.*

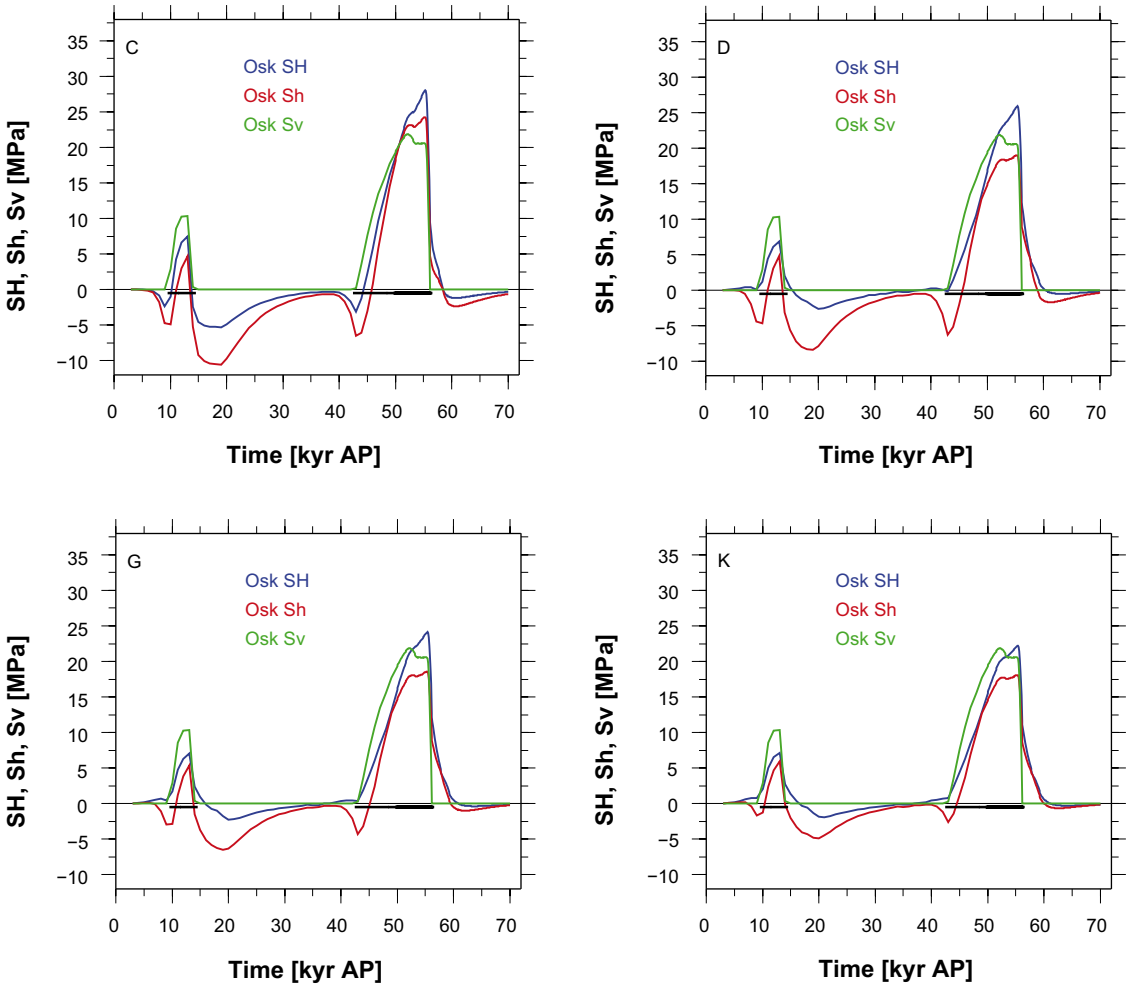

Figure 4-9. *As Figure 4-6, now with models C, D, G, and K which contain density variations.*

4.3.3 Comment

Comparing model C with model A0, we see that lowering the density of the elastic plate reduces the horizontal stresses under the ice load and also the remnant stresses where the ice load were. However, as noted in /Lund 2005a/ the horizontal stresses outside the ice edge are not affected. A lowering of the density acts as a softening of the material, although the density primarily affects the buoyancy of the model through pre-stress advection. Models D, G and K shows, as expected, that lowering the density in combination with compressibility further reduces the horizontal stresses. In model K with the elliptic ice sheet, both SH and Sh are similar in magnitude to the vertical stress under the center of the ice sheet at LGM.

The time histories with the Weichselian ice sheet show similar behavior, Sh is generally lower in magnitude than the vertical stress with the most notable exception being at the end of the glaciation and especially so in Oskarshamn. We see that the horizontal stresses fall off considerably slower in magnitude than does the vertical stress. Sh is generally more tensile in these models than in the uniform density models of section 4.2.

4.4 Viscosity variations

The viscosity of the mantle is of utmost importance in models of glacial isostatic adjustment. Mantle viscosity determines the time frame for the response of the Earth model system and, thus, the amount of plate flexure during a glaciation, the time response of the rebound etc.

Obviously, the induced stresses at any given point in time depend critically on the viscosity of the mantle. Unfortunately, viscosity is the least well determined Earth model parameter discussed thus far. Inferences on mantle viscosity at depth come primarily from GIA studies. Recent studies using GPS and InSAR techniques have also been used to estimate lower crustal and upper mantle viscosities from co-seismic and post-seismic deformation and from modeling of large scale plate motions.

Viscosity estimates for Fennoscandia stem almost entirely from GIA modeling. Recent estimates of upper and lower mantle viscosity are:

- From sea-level data /Lambeck et al. 1998a/:
  Elastic lithosphere 75±10 km, $\eta_{UM} = (3.6\pm1)\cdot10^{20}$ Pa s, from the base of the lithosphere to 670 km depth, and $\eta_{LM} = 8\ (^{-4}\ _{+22})\cdot10^{21}$ Pa s.
- From instrumented sea- and lake-level records /Lambeck et al. 1998b/:
  Elastic lithosphere 80–100 km, $\eta_{UM} = (4–5)\cdot10^{20}$ Pa s, $\eta_{LM} = (3–20)\cdot10^{21}$ Pa s.
- From sea-level histories and a wide variety of data /Kaufmann and Lambeck 2002/:
  $\eta_{UM} = 7\cdot10^{20}$ Pa s, $\eta_{LM} = 20\cdot10^{21}$ Pa s.
- From Scandinavian GPS observations /Milne et al. 2004/:
  Elastic lithosphere 120 km (90–170 km), $\eta_{UM} = 8\ (5–10)\cdot10^{20}$ Pa s, $\eta_{LM} = 10\ (5–50)\cdot10^{21}$ Pa s.
  The values in parenthesis is the 95% confidence limits.

/Milne et al. 2004/ showed that when only the vertical components of the GPS data are taken into account, a model with one mantel viscosity of $(2–3)\cdot10^{21}$ Pa s fit the data as well as the two layer model. The 3D GPS rates, however, require a two layered mantle.

Currently, my finite element models with a multi-layered viscosity structure needs further verification. I will include here the results of model O but with an explicit caution on the reliability of the results. Model KL1 is used as a reliable example of how the stress response changes when a different viscosity is used for the entire mantle. It has a viscosity of $5\cdot10^{21}$ Pa s instead of the reference viscosity of $1\cdot10^{21}$ Pa s. Both KL1 and O are compressible and have density variations.

4.4.1 Elliptical ice sheet

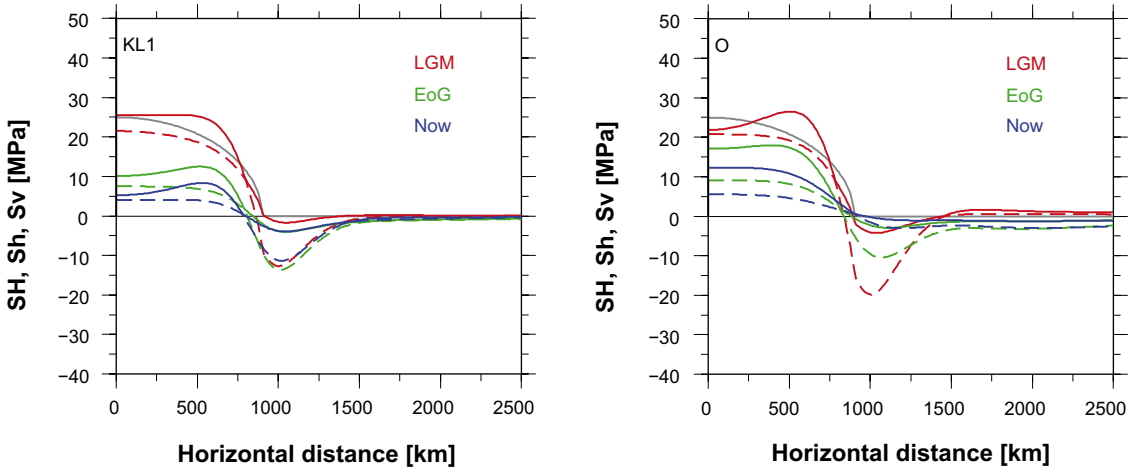

Figure 4-10. *As in Figure 4-7, now with mantle viscosity $5\cdot10^{21}$ Pa s, model KL1, and a two layer viscosity profile (see section 3) in model O.*

4.4.2 Weichselian ice sheet

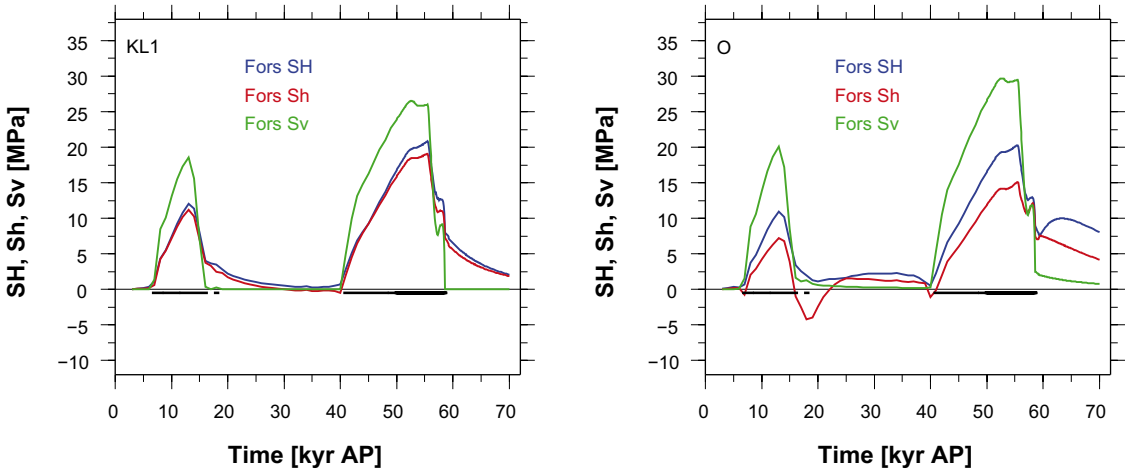

Figure 4-11. *As in Figure 4-8, now with mantle viscosity $5 \cdot 10^{21}$ Pa s, model KL1, and a two layer viscosity profile (see section 3) in model O.*

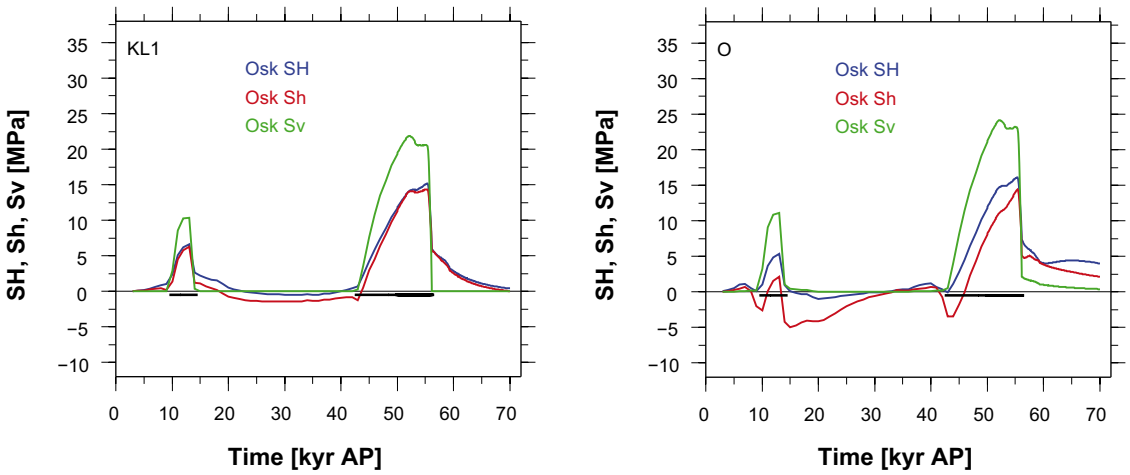

Figure 4-12. *As in Figure 4-9, now with mantle viscosity $5 \cdot 10^{21}$ Pa s, model KL1, and a two layer viscosity profile (see section 3) in model O.*

4.4.3 Comment

Comparing the response of model KL1 to the elliptic ice sheet, Figure 4-10, with that of model K, Figure 4-7, we see that the higher viscosity mantle of KL1 does not allow SH at LGM to reach the magnitudes of SH in model K. After deglaciation, however, the slower response of the high viscosity model KL1 maintain higher stress levels longer than in model K. This slow response becomes very clear in the Weichsel ice simulations in Figures 4-11 and 4-12. We see that the horizontal stresses do not reach the magnitudes of the vertical stress, however, the horizontal stresses are maintained in the model into the current time. Model O is similar to model KL1 in the delayed response, however, the horizontal stresses are questionably high in the elliptical model at later times, and the large remaining horizontal stresses in the Weichsel simulations may also be spurious. The multi-layered viscosity modeling does need further verification work.

4.5 Direction of the horizontal stresses

I have hitherto only discussed the magnitudes of the horizontal stresses and not their directions. The careful reader will have noticed that the directions of SH and Sh does change rather abruptly with the large scale variations in the ice load. In Figure 4-13 we see the horizontal stress directions resulting from model K and the two ice sheets. 0 or 180 degrees is along the profile, i.e. perpendicular to the ice front and approximately in the north-south direction for the Weichselian ice sheet. Consequently, 90 degrees is perpendicular to the profile and along the ice front. These results are very stable, all models produce almost identical directions of horizontal stress, except for some small variations far outside the ice rim where the glacially induced stresses are very small.

Figure 4-13 shows that SH is generally in the direction of the profile under the ice cover (except for at present time centrally under the former ice) but that it changes direction approximately 100 km before the ice edge. SH stays parallel to the ice front out past the fore-bulge and then turn parallel to the profile again. Considering the time histories at Forsmark and Oskarshamn, we see that SH is generally perpendicular to the profile until there is significant ice growth over the area. When the ice grows, SH turns parallel to the profile until deglaciation initiates, when it again turns perpendicular to the profile. As the Weichsel ice profile is oriented slightly north-northeast, the along-profile direction is sub-parallel to the direction of least horizontal tectonic stress in southern Sweden /Slunga 1991, Lund and Zoback 1999/ and the profile-perpendicular direction, therefore, sub-parallel to the direction of maximum horizontal tectonic stress. The maximum glacially induced stress will, thus, reinforce the tectonic minimum horizontal stress during the ice covered periods.

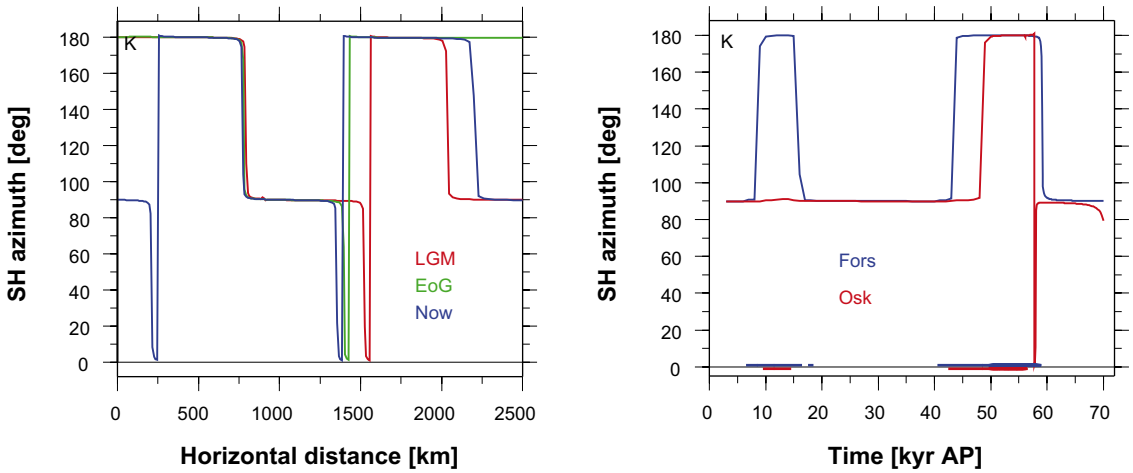

Figure 4-13. *Direction of the maximum horizontal stress, SH, using Earth model K. 0 or 180 degrees is the along-profile direction, 90 degrees the profile-perpendicular direction. Left, the elliptical ice model is used to display the direction of SH along the ice profile at three different times, last glacial maximum (red), end of glaciation (green) and current (blue). Right, the Weichsel ice model is used to plot time histories at Forsmark (blue) and Oskarshamn (red).*

4.6 Fault stability in Forsmark and Oskarshamn

Knowing the stresses induced by the glaciation we can proceed to infer how the ice sheet affects the stability of faults in the crust. Fault stability during glaciation can be assessed using a number of different techniques, e.g. /Johnston 1987, Wu and Hasegawa 1996, Ivins et al. 2003, Lund 2005a/, common to these is the application of a failure criterion to the estimated stress state. I will follow the methodology presented in /Lund 2005a/ and use the Mohr-Coloumb failure criterion as the basis of a fault stability assessment scheme. The Mohr-Coloumb criterion relates the shear stress τ on a fault plane to the normal stress σ_n via the coefficient of friction μ.

$$\tau = \mu(\sigma_n - P_f) + S_0$$

where P_f is the pore fluid pressure and S_0 the cohesion. I define instability as

$$I = \tau - \mu(\sigma_n - P_f) - S_0$$

and we see that if I is positive, the shear stress is larger than the frictional force and the fault will fail in frictional sliding, possibly as an earthquake. When considering background faults at depth in the crust, the cohesion term is insignificant and usually ignored /Brace and Kohlstedt 1980, Zoback and Healy 1984/. Here, I am evaluating fault stability at the intended repository depth of 500 m and the cohesion term could be of significance. However, as I currently have no site specific data on cohesion, or rock types, I will ignore the cohesion for now. The coefficient of friction is generally independent of rock type and laboratory measurements indicate a value of approximately 0.5–0.9 /Byerlee 1978/.

The glacial stresses modify the background tectonic stress field and both stress fields have to be taken into account for a correct assessment of fault stability. How the background stress field is modeled depend on the available data. There are three different lines of evidence indicating that the intraplate, continental upper crust is in a state of failure equilibrium on optimally oriented faults, see summary in /Zoback and Townend 2001/. 1) Seismicity induced by fluid injection or reservoir impoundment; 2) Earthquakes triggering other earthquakes; 3) In situ stress measurements in deep boreholes. Additionally, crustal stress measurements consistently agree with predictions of stress based on Coulomb frictional failure theory, using laboratory derived coefficients of friction. Shallow stress measurements indicate, however, that the state of stress at 500 m depth can vary considerably even over relatively short distances and may not be in failure equilibrium. In this study I will utilize stress measurement from the site investigations in Forsmark and Oskarshamn, assume that the rock mass is in failure equilibrium (we do have occasional earthquakes in the areas, see /Bödvarsson et al. 2006/) and calculate the corresponding coefficient of friction. I will then use this equilibrium state of stress as the reference stress state, apply the induced glacial stresses to it and follow the development of stability over time.

Pore fluid pressure is a vital component of fault stability assessment. Nevertheless, in the following I will ignore pore pressure since its inclusion in the glacial context is slightly involved and not within the scope of this study.

4.6.1 The state of stress in Forsmark and Oskarshamn

The ongoing site investigations in Forsmark and Oskarshamn produce site specific models of a large variety of parameters, including the state of stress. The following is the result of site models version 1.2. For Oskarshamn I use the Laxemar 1.2 model.

Forsmark

Stress data for Forsmark is obtained from /SKB 2005/ pg. 291. The state of stress at 500 m depth is assumed to be purely Andersonian, with one vertical and two horizontal components. The maximum principal stress, S1, is horizontal, directed N142°E and has magnitude 45 MPa. The intermediate principal stress, S2, is also horizontal, with magnitude 18 MPa and the minimum principal stress, S3, is vertical and 13 MPa in magnitude. Forsmark is, thus, characterized by a reverse faulting state of stress at 500 m depth and faults dipping 30° to the NW or SE will be optimally oriented for failure, with slip in the up-dip direction. Ignoring pore pressure and cohesion, the stress state in Forsmark is in frictional equilibrium with a coefficient of friction of 0.66.

Oskarshamn (Laxemar)

The Laxemar area is characterized by two distinct stress states in two different spatial domains, according to /SKB 2006a/ pg. 239. At 500 m depth, state I has S1 = 34 MPa, horizontal in the direction N132°E, S2 = 13.5 MPa vertical and S3 = 10 MPa horizontal. State II is a lower magnitude stress state with S1 = 16 MPa horizontal in the direction N132°E, S2 = 13.5 MPa vertical and S3 = 5 MPa horizontal. Both these stress states are strike-slip faulting states of stress, i.e. vertical faults striking E-W or NNW-SSE are optimally oriented for failure, with slip in the horizontal direction. Ignoring pore pressure and cohesion, the state of stress in Laxemar is in frictional equilibrium with a coefficient of friction of 0.65 for state I and 0.61 for state II. In the modeling below I have used the Laxemar I state of stress.

4.6.2 Modeling fault stability

The principal stresses from the site investigations are added to the glacial stresses, after a coordinate transformation to the local profile coordinate system. The combined stresses are then assessed with the instability criterion above (without pore pressure or cohesion) and a time history of fault stability is produced. Below I show the fault stability histories for models K, Q and KL1.

We see in Figure 4-14 that faults in the Forsmark area are relatively more stable than their Oskarshamn counterparts. Only in the early stages of deglaciation, at approximately 17 kyr AP and 59 kyr AP, does the Forsmark area experience unstable fault conditions. In Oskarshamn, on the contrary, fault instability is prevalent during much of the inter-stadial between 15–35 kyr AP. The magnitude of instability can be seen to be model dependent but the time duration is relatively constant, although the high viscosity model KL1 significantly reduces the instability in Oskarshamn after the 15 kyr AP deglaciation.

What is then the cause of the large difference in fault stability between the two proposed repository sites? The main component is the background stress field. We see that during times of ice cover, both the Forsmark reverse faulting regime and the Oskarshamn strike-slip state are stabilized. The Oskarshamn strike-slip state is, however, much more sensitive to the glacially induced stresses outside the ice edge. We see that both growing and retreating ice conditions induce instability in Oskarshamn. Comparing the end of the stadial at ~15 kyr AP with the conditions at the end of the glaciation, we note, however, that there are additional variables that affect fault stability in Oskarshamn. In order to better understand the differences in fault stability between Forsmark and Oskarshamn, I plot vertical displacements and stresses, the glacially induced as well as the total stress state, all along the 2D profile.

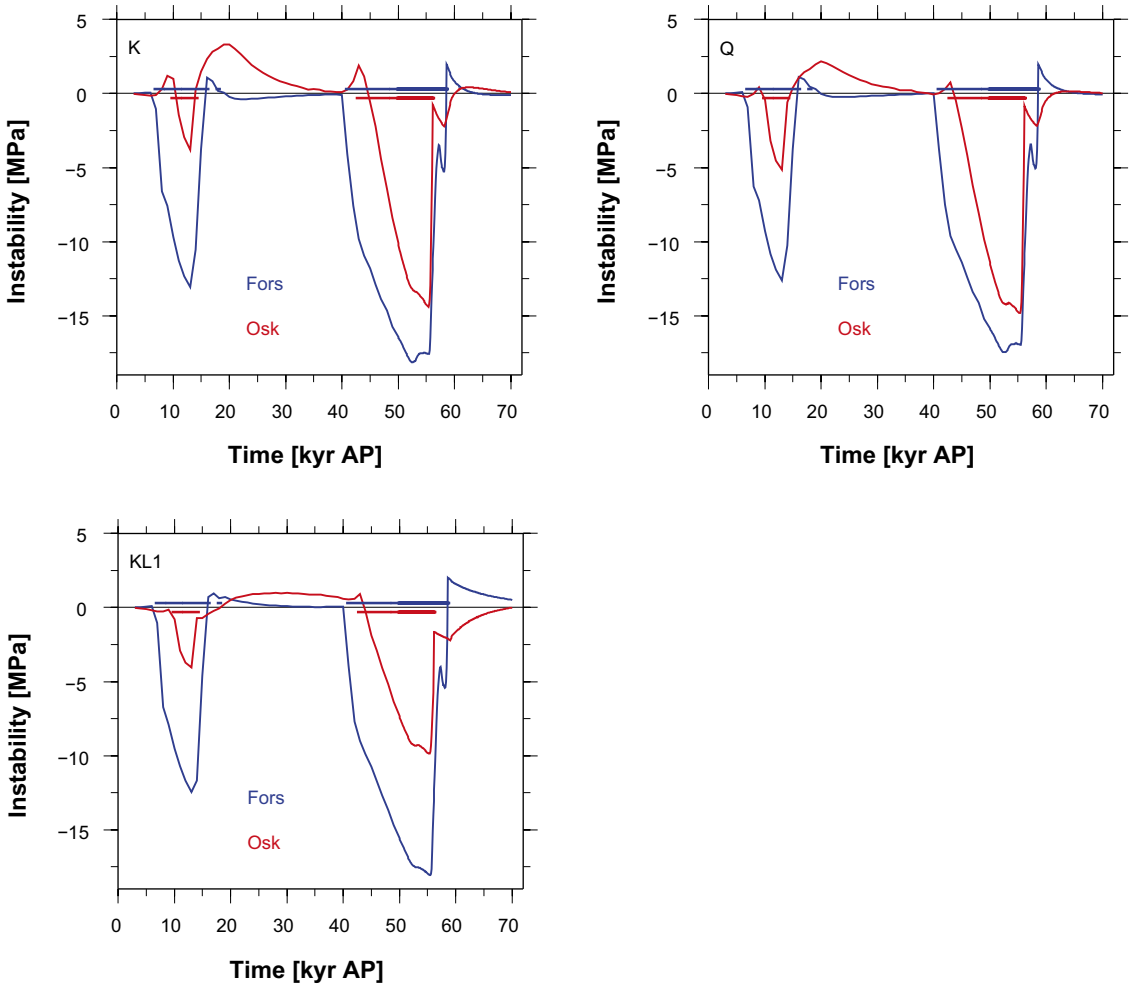

Figure 4-14. *Stability time histories for models K, Q and KL1. Instability larger than zero implies unstable conditions and likely fault failure. The Weichselian ice model has been used and reference stresses from Forsmark and Oskarshamn. Forsmark stability in blue, Oskarshamn in red. Blue and red horizontal lines around zero indicate the times of ice cover at Forsmark and Oskarshamn, respectively.*

We see in Figure 4-15 that at 20 kyr AP Oskarshamn is in the fore-bulge area and although both glacially induced horizontal stresses are tensional, they have different magnitudes which increases the shear stress available for fault instability in a strike-slip environment, see the right panels in Figures 4-16 and 4-17. Note that the orientation of the horizontal stresses is important in this case as it determines how they add together. At 59 kyr AP, Oskarshamn is still situated well into the glacial depression and does not experience tensional glacial stresses or even significant differences in the induced stresses, i.e. faults are stable. Analyzing Forsmark at 20 kyr AP we see in Figure 4-15 that although Forsmark is within the glacial bowl, the induced horizontal stresses are tensional and significantly different. However, since Forsmark has a reverse faulting environment, it is the difference between the vertical stress and the maximum horizontal stress which determines fault stability, and this difference is barely affected since the induced SH is close to zero. Forsmark thus remains stable, or rather at equilibrium. At 59 kyr AP Forsmark experiences large horizontal stresses and as the ice has recently left the area, see Figure 2-3, decreasing the vertical stress to the background state, fault instability develops. At 43 kyr AP, on the contrary, there is enough ice coverage over Forsmark to balance the increased horizontal stresses.

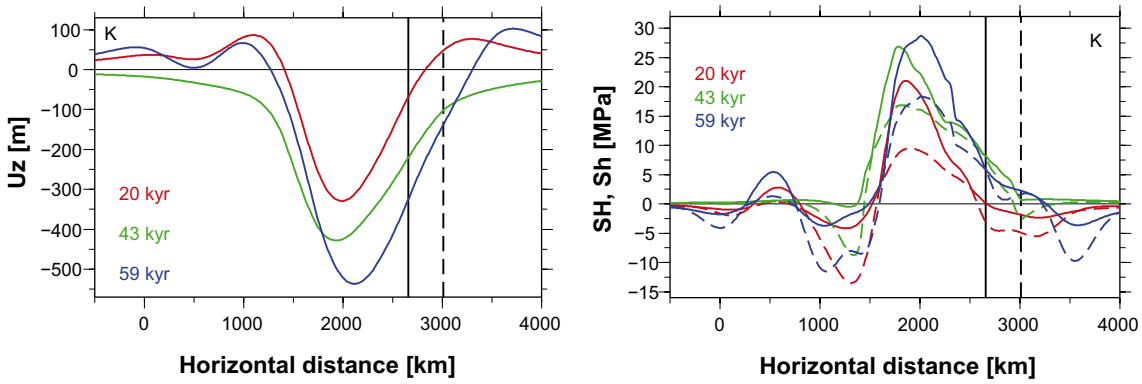

Figure 4-15. *Profiles through the entire length of the Weichselian ice sheet model using Earth model K. The profile runs from north to south, at 14.9° angle to a north-south meridian, and horizontal distance zero is just north of the ice. The maximum extent of the ice sheet at LGM, cf Figure 2-2, is from 60–3,550 km. Shown are three times during the glaciation, 20 kyr AP (red), 43 kyr AP (green) and 59 kyr AP (blue). The solid black vertical line shows the location of Forsmark, the dashed vertical line the location of Oskarshamn along the profile. Left) Vertical displacements. Right) Maximum glacially induced horizontal stress, SH (solid lines) and minimum glacially induced horizontal stress, Sh (dashed lines).*

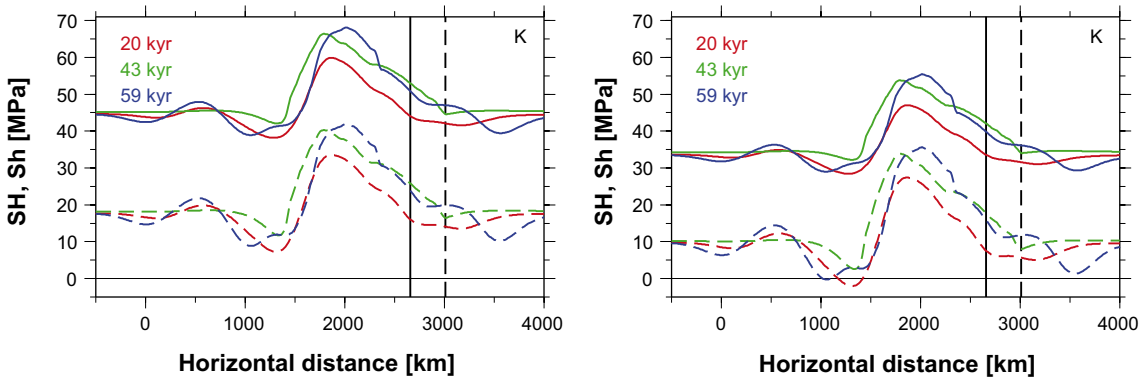

Figure 4-16. *As in Figure 4-15, Left) SH (solid line) and Sh (dashed line) for the glacially induced stresses plus the background state of stress at Forsmark. Right) SH (solid line) and Sh (dashed line) for the glacially induced stresses plus the background stress state I at Laxemar, Oskarshamn.*

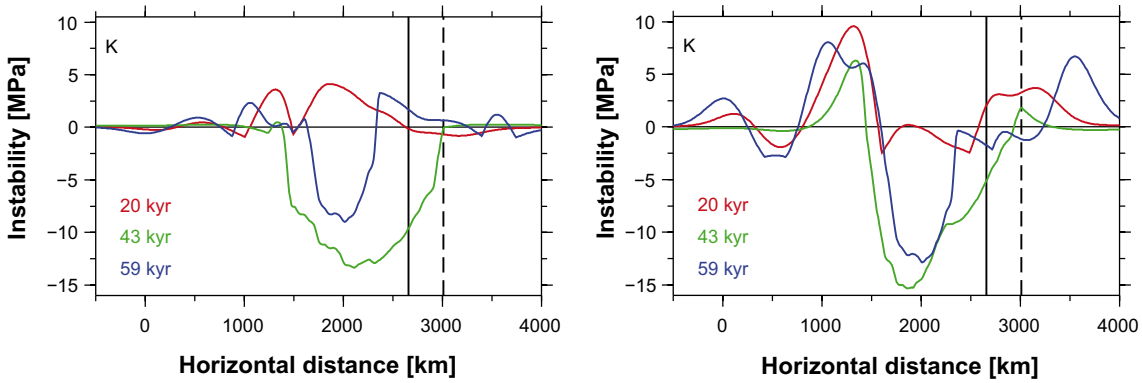

Figure 4-17. *As Figure 4-15, Left) Fault instability, using the background state of stress at Forsmark for the entire profile. Right) Fault instability, using the background stress state I at Laxemar, Oskarshamn for the entire profile.*

5 Discussion

This study shows that as the complexity of the elastic properties of the Earth model is increased from very simple, large scale average models to more realistic representations of the Earth, the induced horizontal stress magnitudes generally decrease close to the Earth's surface. This is due to a general softening of the surface layer as it is less affected by deeper, stiffer properties. From the simple A0 reference model to the complex K or Q models, the induced horizontal stresses decreased by approximately a factor one-third. Variations in elastic properties slightly alters the shape of the stress functions in space and time, but the differences do usually not affect the general conclusions about the induced stresses. Instead, other parameters in the modeling have much larger influence on the resulting stresses. One such parameter is viscosity, and we saw above that it affects both stress magnitudes and the temporal behavior of the stresses significantly. Since inferences on viscosity are difficult to make without relatively large uncertainties, this will affect the variance of the stresses in the models. There are, however, other larger sources of model uncertainty.

- The ice model. The ice model drives the deformation and is, therefore, of utmost importance. We have seen how both the thickness, extent and duration of the ice sheet affects the response of the Earth model in the comparative studies of Forsmark and Oskarshamn. It is obvious that the ice model differences depicted in Figure 2-3 will have a profound influence on the induced stress levels. /Lambeck 2005/ presents induced stresses in Forsmark and Oskarshamn for one particular Earth model, and they are generally similar in magnitude to the stresses presented here, but have very different temporal variation.
- The 2D modeling. Ignoring the three-dimensionality of the ice model will undoubtedly affect the estimated stresses. Even though the ice sheet in very general terms grows from northern Scandinavia southward, and retreats in the opposite direction, a 2D profile will usually not estimate all three principal stresses correctly. The 3D ice model of /Lambeck 2005/ show, for example, that the maximum horizontal stress at Forsmark and Oskarshamn are generally oriented perpendicular to each other at any one point in time.
- Horizontal layers in the Earth. In the north-south direction through much of Sweden an approximation of subhorizontal material layers in the Earth is reasonable. However, there are major transitions in lithospheric structure to the south and similarly off the coast of Scandinavia to the north. Considering the east-west direction, an assumption of subhorizontal layering is clearly inappropriate as the lithosphere thickens considerably from the ocean off the coast of Norway to the thick craton of central Finland. Preliminary modeling shows that such lateral thickness variations potentially influence the stress distribution considerably, concentrating stress in some areas and decreasing it in other.
- Modeling simplifications. The models presented here are simplifications of the underlying physical system. I have ignored the effect of varying water load as the ice sheet increase or decrease. /Milne et al. 2004/ show that this sea-level component of GIA modeling amounts to approximately 10% of the model response (in terms of deformation rates). The exclusion of compressibility induced buoyancy and the effects of density variations on gravity also influence the results, although these are second order effects.

5.1 Fault stability

In my discussion of fault stability I have excluded the pore pressure. This is a significant omission as pore pressure has a very large effect on the strength of faults. Including pore pressure in the glacial context is, however, a non-trivial exercise. Pressure conditions under an ice sheet

vary considerably both on an annual basis and with location. Simplifications, such as assuming either hydrostatic conditions through the entire thickness of the ice sheet, or water only below the glacier, can be made to ease a modeling effort.

At the relatively shallow depth of investigation for a nuclear waste repository, 500 m, the effect of including the cohesion of faults in the stability assessment should probably be investigated. Ignoring cohesion could possibly lead to inferences of more unstable fault conditions than what a full analysis would show.

It is interesting to note that although stress magnitudes vary in the various models of this study, fault stability calculations based on these models are generally very similar, albeit with different magnitudes. This is in part due to the background stress field and in part due to the ice model, which is the same for all models. In this context, it is interesting to compare the current study to the results of /Lambeck 2005/ and /Lund 2005b/, which both used the ice sheet of /Lambeck 2005/ to infer stabilities at Forsmark and Oskarshamn. Using a general, reverse faulting background state of stress in frictional equilibrium for Forsmark, /Lund 2005b/ obtained fault stabilities very similar to those in this study where the only period of instability is right at the end of the glaciation. For Oskarshamn, using a strike-slip state of stress, a very large magnitude peak of instability was inferred at 50 kyr BP as Oskarshamn entered the fore-bulge of the growing ice sheet. Fault instability at Oskarshamn mid-way through the glacial cycle may, therefore, be an issue that should be investigated further.

6 Conclusions

This study has considered the response to a glaciation of Earth models of increasingly complex structure in elastic parameters and viscosity. The models are one-dimensional in the sense that they vary only in the depth direction, i.e. there are only uniform, horizontal layers in the models. I find that as the complexity of the models increase, and the properties of the uppermost kilometer of the Earth become less affected by average properties from deeper down, the flexural stresses at 500 m depth decrease, as expected. A lower Young's modulus, lower compressibility and lower density in the uppermost layer all act to lower the stresses. However, the three properties act differently on the resulting response. Introducing layering in Young's modulus generally decreases the stresses all along a profile through the ice model. Going from incompressible to compressible models affect the stresses outside the ice edge significantly more than the stresses under the ice sheet. Introducing layering in density conversely affect the stresses under the ice sheet more than those outside the ice edge. The combined effects of the most complex models tested here show that the glacially induced horizontal stresses at 500 m depth decrease to levels very similar in magnitude to the loading stress. There are, however, temporal variations in these horizontal stresses that do not follow the loading stress and which induce tensional or compressional horizontal stresses that persist when no ice is present.

As is well known, changes in viscosity structure has a very large effect on the Earth response. Viscosity affect both the magnitudes of the induced stresses and the temporal behavior of the stress evolution. This is confirmed in the current study.

The glacially induced stresses for some of the models have been used in combination with the current background stress field at Forsmark and Oskarshamn, as estimated in SKB's site models /SKB 2005, 2006a/, to evaluate fault stability throughout a glacial cycle. The results show that with the used ice model and Earth models, fault stability is generally enhanced in both Forsmark and Oskarshamn during ice cover of the sites. Oskarshamn, however, show long periods of decreased fault stability during inter-stadials and for some models at the end of the final deglaciation. Fault stability in Forsmark is generally higher than in Oskarshamn, with the exception of a pulse of instability at the end of deglaciations.

7 References

ABAQUS, 2004. ABAQUS manuals, version 6.5, ABAQUS, Inc., www.abaqus.com.

Brace W F, Kohlstedt D L, 1980. Limits on lithospheric stress imposed by laboratory experiments, J. Geophys. Res., 85, 6,248–6,252.

Byerlee J D, 1978. Friction of rocks, Pure Appl. Geophys., 116, 615–626.

Bödvarsson R, Lund B, Roberts R, Slunga R, 2006. Earthquake activity in Sweden, R-06-67, Svensk Kärnbränslehantering AB.

Dziewonski A M, Anderson D L, 1981. Preliminary reference Earth model, Phys. Earth Planet. Inter., 25, 297–356.

Han D, Wahr J, 1995. The viscoelastic relaxation of a realistically stratified Earth, and a further analysis of postglacial rebound, Geophys. J. Int., 120, 287–311.

Ivins E R, James T S, Klemann V, 2003. Glacial isostatic stress shadowing by the Antarctic ice sheet, J. Geophys. Res., 108, 2560, doi: 10.1029/2002JB002182.

Johnston A C, 1987. Suppression of earthquakes by large continental ice sheets, Nature, 330, 467–469.

Johnston P, 1993. The effect of spatially non-uniform water loads on predictions of sea-level change, Geophys. J. Int., 114, 615–634.

Johnston P, Wu P, Lambeck K, 1998. Dependence of horizontal stress magnitude on load dimension in glacial rebound models, Geophys. J. Int., 132, 41–60.

Kaufmann G, Lambeck K, 2000. Mantle dynamics, postglacial rebound and the radial viscosity profile, Phys. Earth Planet Inter., 121, 301–324.

Klemann V, Wolf D, 1998. Modelling of stresses in the Fennoscandian lithosphere induced by Pleistocene glaciations, Tectonophysics, 294, 291–303.

Klemann V, Wolf D, 1999. Implications of a ductile crustal layer for the deformation caused by the Fennoscandian ice sheet, Geophys. J. Int., 139, 216–226.

Klemann V, Wu P, Wolf D, 2003. Compressible viscoelasticity: stability of solutions for homogeneous plane earth models, Geophys. J. Int., 153, 569–585.

Lambeck K, Smither C, Johnston P, 1998a. Sea-level change, glacial rebound and mantle viscosity for northern Europe, Geophys. J. Int., 134, 102–144.

Lambeck K, Smither C, Ekman M, 1998b. Tests of glacial rebound models for Fennoscandinavia based on instrumented sea- and lake-level records, Geophys. J. Int., 135, 375–387.

Lambeck K, 2005. Glacial load stresses: Can existing faults or other zones of crustal weakness be reactivated during glacial cycles?, in Expert Panel Elicitation of Seismicity Following Glaciation in Sweden, eds. S. Hora and M. Jensen, SSI_Report 2005:20, Swedish Radiation Protection Authority, Stockholm Sweden.

Latychev L, Mitrovica J X, Tromp J, Tamisiea M E, Komatitsch D, Christara C C, 2005. Glacial isostatic adjustment on 3-D Earth models: a finite volume formulation, Geophys. J. Int., 161, 421–444, doi: 10.1111/j.1365-246X.2005.02536.x.

Lund B, Zoback M D, 1999. Orientation and magnitude of in situ stress to 6.5 km depth in the Baltic Shield, Int. J. Rock. Mech. Min. Sci., 36, 169–190.

Lund B, 2005a. Effects of deglaciation on the crustal stress field and implications for endglacial faulting: A parametric study of simple Earth and ice models, TR-05-04, Svensk Kärnbränslehantering AB.

Lund B, 2005b. Large earthquakes during a glacial cycle, in Expert Panel Elicitation of Seismicity Following Glaciation in Sweden, eds. S. Hora and M. Jensen, SSI 2005:20, Swedish Radiation Protection Authority, Stockholm Sweden.

Martinec Z, 2000. Spectral-finite element approach to three-dimensional viscoelastic relaxation in a spherical earth, Geophys. J. Int., 142, 117–141.

Milne G A, Mitrovica J X, 1998. Postglacial sea-level change on a rotating Earth, Geophys. J. Int., 133, 1–19.

Milne G A, Mitrovica J X, Scherneck H-G, Davis J L, Johansson J M, Koivula H, Vermeer M, 2004. Continuous GPS measurements of postglacial adjustment in Fennoscandia: 2. Modeling results, J. Geophys. Res., 109, B02412, doi: 10.1029/2003JB002619.

Mitrovica J X, Milne G A, Davis J L, 2001. Glacial isostatic adjustment on a rotating Earth, Geophys. J. Int., 147, 562–578.

Näslund J-O, 2006. Ice sheet dynamics, in Climate and climate related issues for the safety assessment SR-Can, TR-06-23, Svensk Kärnbränslehantering AB.

Peltier W R, 1974. The impulse response of a Maxwell Earth, Rev. Geophys. Space Phys., 12, 649–669.

SKB, 2005. Preliminary site description, Forsmark area – version 1.2, R-05-18, Svensk Kärnbränslehantering AB.

SKB, 2006a. Preliminary site description, Laxemar sub-area – version 1.2, R-06-10, Svensk Kärnbränslehantering AB.

SKB, 2006b. Climate and climate related issues for the safety assessment SR-Can, TR-06-23, Svensk Kärnbränslehantering AB.

Slunga R, 1991. The Baltic Shield earthquakes, Tectonophysics, 189, 323–331.

Wolf D, 1991. Viscoelastodynamics of a stratified, compressible planet: incremental field equations and short- and long-time asymptotes, Geophys. J. Int., 104, 401–417.

Wu P, Peltier W R, 1982. Viscous gravitational relaxation, Geophys. J. R. astro. Soc., 70, 435–485.

Wu P, 1992. Deformation of an incompressible viscoelastic flat earth with power-law creep: a finite element approach, Geophys. J. Int., 108, 35–51.

Wu P, Hasegawa H S, 1996. Induced stresses and fault potential in eastern Canada due to a disc load: a preliminary analysis, Geophys. J. Int., 125, 415–430.

Wu P, Ni Z, 1996. Some analytical solutions for the viscoelastic gravitational relaxation of a two-layer non-self-gravitating incompressible spherical earth. Geophys. J. Int., 126, 413–436.

Wu P, van der Wal W, 2003. Postglacial Sealevels on a Spherical, Self-gravitating Viscoelastic Earth: Effects of lateral viscosity variations in the upper mantle on the inference of viscosity contrasts in the lower mantle, Earth and Planet. Sci. Lett., 211, 57–68.

Wu P, 2004. Using commercial finite element packages for the study of earth deformations, sea levels and the state of stress, Geophys. J. Int., 158, 401–408.

Zoback M D, Healy J H, 1984. Friction, faulting and in situ stress, Ann. Geophys., 2, 689–698.

Zoback M D, Townend J, 2001. Implications of hydrostatic pore pressures and high crustal strength for the deformation of intraplate lithosphere, Tectonophysics, 336, 19–30.